Proceedings of the American Control Conference
Anchorage, AK May 8-10, 2002

Coarse Gain Recurrent Integrator Model for Sensorimotor Cortical Command Generation

Ola Ayaso, Steve G. Massaquoi, Munther Dahleh
Sensorimotor Control Project
Laboratory for Information and Decision Systems, Artificial Intelligence Laboratory, and HST Division,
Massachusetts Institute of Technology

Abstract

The coarsely sampled inverse Jacobian, or "Coarse Gain" Recurrent Integrator Command Generator (CGRICG) model* is a preliminary proposal for motor command generation in the sensorimotor cortex during unloaded horizontal reaching movements based significantly upon implicit coordinate transformation. The core of the model is an integrator that in negative feedback configuration performs approximate differentiation of a central movement trajectory command. Together with an accurate forward kinematic model and a distribution and scaling network that is only coarsely tuned in relation to movement direction, the feedback configuration achieves inverse kinematic transformation implicitly throughout the workspace. Simulations of the CGRICG directing motion of a six-muscle, two-joint arm model reproduce gross kinematic features of human and primate arm movement as well as plausible neurophysiological signals in internal sensorimotor cortical neurons. The CGRICG model suggests that cortical network connection strengths may be adapted to improve straightness of motion without affecting final target location.

1 Introduction

Though the importance of the sensorimotor cortex in generating commands for limb muscles during voluntary movements is well established, the variables that the sensorimotor cortex encodes and how the motor cortical signals are used to control and command motor systems to execute even the simplest tasks, such as point-to-point hand movements, are not known. The input signals to sensory cortex and output signals from the motor cortex and their correlations with task variables such the position of the limb in space, speed of motion of the limb, or force exerted on that limb have been measured by many [5, 8, 13]. But these correlations do not necessarily imply causal or controlling relationships. What is needed, and is suggested here, is a physiologically plausible model that can explain the command generating mechanism of the motor cortex in view of the signals that are needed by the muscles of the limb.

From the perspective of control, the biological system under investigation consists of a plant, defined as the arm and local (cervical) levels of the spinal cord, a dynamic compensator representing the action of the anterior cerebellum (CBLLM), and a command generator consisting of the broadly considered sensorimotor cortical areas of the brain (Figure 1). The various other components of the complex multi-loop biological motor control system, such as thalamus and basal ganglia, are not represented explicitly or investigated here.

2 The Compensated Plant Model

The two-joint arm (Figures 1 and 2), is composed of the passive skeleton, modeled as rigid links, and the muscles (actuators) that receive an activating signal, $\mathbf{u}$, from the central nervous system (CNS: brain and spinal cord) and accordingly generate the torques required at the two joints. We follow the equilibrium point hypothesis which proposes that the viscoelastic properties of muscle enable the arm to follow the "virtual" equilibrium trajectory [2, 6, 7, 21] specified by $\mathbf{u}$. The resultant model, similar to that used by others [15, 21, 17], is of only modest complexity but retains the salient dynamic characteristics of the human/primate limb.

The state space representation of the six-muscle arm as it behaves when the dynamic compensation of the cerebellum is taken into account (Figure 3):

$$\begin{bmatrix} \dot{q}_1 \\ \dot{q}_2 \end{bmatrix} = \begin{bmatrix} 0 & I \\ -H^{-1}R(u,q_1) & -H^{-1}(D(u,q_1,q_2)+C(q_1,q_2)) \end{bmatrix} \begin{bmatrix} q_1 \\ q_2 \end{bmatrix} + \begin{bmatrix} 0 & 0 \\ H^{-1}R(u,q_1) & H^{-1}D(u,q_1,q_2) \end{bmatrix} \begin{bmatrix} q_{1_c} \\ q_{2_c} \end{bmatrix}$$

where $q_1 = \Theta$, $q_2 = \dot{\Theta}$, $q_{1_c} = \Theta_c = \begin{bmatrix} \theta_{c_s} & \theta_{c_e} \end{bmatrix}'$, $q_{2_c} = \dot{\Theta}_c = \begin{bmatrix} \dot{\theta}_{c_s} & \dot{\theta}_{c_e} \end{bmatrix}'$. $H = H(\Theta)$ is the 2x2, symmetric configuration-dependent arm inertia matrix, and $C = C(\Theta, \dot{\Theta})$ is the matrix related to centrifugal and Coriolis forces. R and D are the 2x2 matrices that represent net effective nonlinear joint stiffnesses and viscosities, respectively, that are dependent on the arm configuration and level of muscle activation. For the

*This research is supported by an NSF KDI program grant IBN-9873478. The Sensorimotor Control Project is a member of the MIT-Harvard HST NeuroEngineering Research Collaborative. http//hst.mit.edu/nerc/

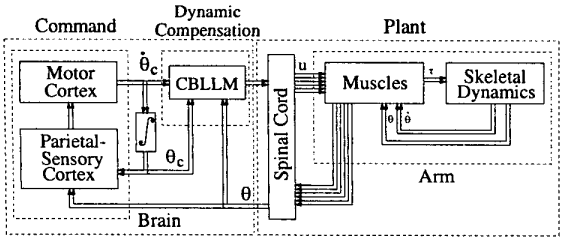

Figure 1: Basic configuration of the biological motor control system.

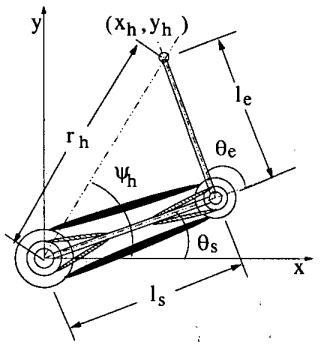

Figure 2: The six-muscle arm.

preliminary simulations examined here, constant approximations to $R(u, q_1)$ and $D(u, q_1, q_2)$ were used†. Not shown in the above state space representation are the low-pass filtering effects associated with muscular activation which were also included in the model.

3 The CGRI Command Generator

The Coarse Gain Recurrent Integrator Command Generator (CGRICG) model is shown in Figure 3 fairly explicitly in terms of its proposed correspondence with brain circuitry. The CGRICG model provides the needed joint position and velocity signals to the compensator-plant model. We consider that a "reference command" network encodes the intended hand trajectory $X_{h_{ref}}(t) = [x_{h_{ref}}(t), y_{h_{ref}}(t)]'$ and projects this the to "predicted kinematic error" neurons. These, taken to reside in parietal area 5 [14, 16], are considered to encode the difference between $X_{h_{ref}}$, and a roughly predicted hand trajectory, $\hat{X}_h = [\hat{x}_h, \hat{y}_h]'$. The latter signal is proposed to be derived from the integrated component of the motor command that is fed back to the motor cortex as a recurrent corollary efferent signal [3]. We postulate that "distribution" neurons, in the motor cortex, scale and allocate the parietal signal appropriately to joint-specific output neurons. We consider that the scaling factors (see equations 5 and 6) may be a substrate for motor learning to improve control of the plant. The site of the proposed integrator has not been established definitively. An attractive candidate is the "reverberatory" brainstem neural circuitry associated with the cerebellum ([1, 12, 17]). The dashed path in Figure 3 represents proprioceptive signals that presumably also participate in, and improve hand position prediction and therefore control (e.g. [17]). This feature was not yet included in current simulations. We note that the model does not include physiological signal transmission delays which can be as great as 20 ms along some of the internal paths shown. A variety of models have been proposed to explain how the CNS, especially the cerebellum, may compensate for these delays [17, 19, 22] and we assume here that sufficient compensation is achieved.

The reference command, kinematic error, distribution, and sensory networks are each built of 8 simple linear units that represent neurons or neuronal assemblies (Figure 4). The networks themselves are designed to have inter-unit connectivities that are broadly consistent with known cerebral cortical micro-architecture. In a target-directed reaching movement, the reference command (RC) network is postulated to represent the intended motion as a vector pointed at the target in the workspace, whose magnitude grows smoothly over time (e.g. Figure 5A). The direction of this vector signal is represented by the distribution of activity among the RC units, while its magnitude corresponds to the overall intensity of firing activity of the population. This "population vector" representation of signals has been found in motor cortex [8] and in parietal area 5 [13, 14, 16]. However, it is not clear yet that these subpopulations have the postulated time course of activity during motion and this remains a point for future investigation. In any case, each RC unit, r_k, is taken to be principally responsible for commanding movement in a specific direction, $\hat{\phi}_k$, with the 8 $\angle \hat{\phi}_k$ distributed uniformly from 0 to $7\pi/4$. The activity of each RC unit, and therefore output signal to the predicted kinematic error (KE) network, is then determined by the projection of $X_{h_{ref}}$ onto $\hat{\phi}_k$ resulting in a broad distribution of activity within the network consistent with the experimentally observed cosine tuning curves of population vectors [8]. Similarly, each sensory (S) network unit s_l is principally responsible for encoding prediction and movement-related signals in specific uniformly separated nominal directions, $\hat{\phi}_l$. The output of each s_l, is determined by the component of $\hat{X}_h$ along $\hat{\phi}_l$. The output firing rate of a given KE network unit, e_j, is taken to be a linear combination of the firing rates of its inputs from RC, S, and neighboring KE units:

$$e_j = \sum_i w_{ij} e_i + \sum_k v_{kj} r_k + \sum_l u_{lj} s_l \qquad (1)$$

where w_{ij}, v_{kj}, and u_{lj} are synaptic strengths (connection weights).

To set the weights, each KE neuron was first assigned a nominal direction $\hat{\xi}$. The v_{kj} were determined such that excitatory connections are strongest between RC

†See appendix for the numerical values used in simulations.

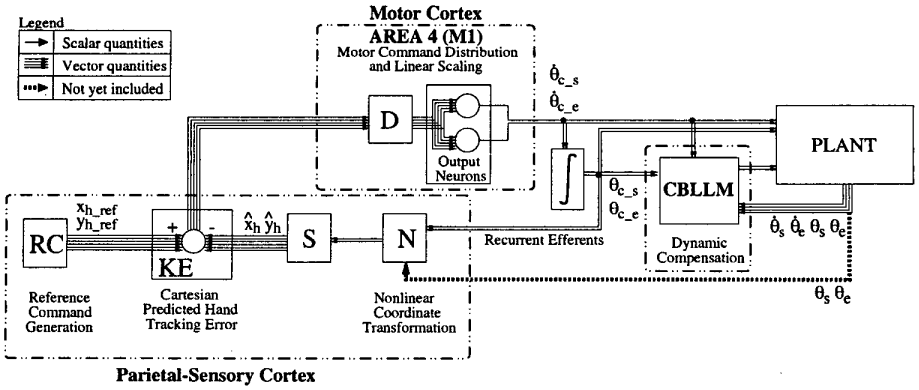

Figure 3: Current CGRICG-Compensator-Plant model (solid paths).

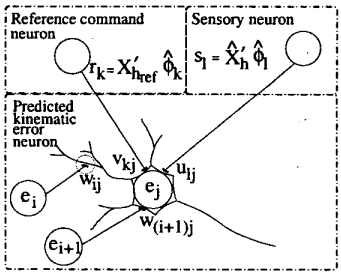

Figure 4: Neuronal unit connections.

and KE units having closely aligned nominal directions, and weakest when these directions are very different:

$$v_{kj} = c_v \exp\{-\frac{(\angle\hat{\xi}_j - \angle\hat{\phi}_k)^2}{2{\sigma_v}^2}\} \quad (2)$$

where c_v and σ_v are arbitrary shaping constants.

The u_{lj}, on the other hand, were determined such that excitatory connections are strongest between S and KE units having *opposite* nominal directions, and weakest when these directions are closely aligned:

$$u_{lj} = c_u \exp\{-\frac{(\angle\hat{\xi}_j - \angle\hat{\phi}_k + \pi)^2}{2{\sigma_u}^2}\} \quad (3)$$

where c_u and σ_u are constants.

The w_{ij} were then determined analogously in the KE population. Here, the effects of both excitatory and inhibitory local connections are included as are seen in cerebral cortex [9]. These are implemented using two different Gaussian functions of angular separation:

$$w_{ij} = k_E \exp\{-\frac{(\angle\hat{\xi}_j - \angle\hat{\xi}_i)^2}{2{\sigma_E}^2}\} - k_I \exp\{-\frac{(\angle\hat{\xi}_j - \angle\hat{\xi}_i)^2}{2{\sigma_I}^2}\} \quad (4)$$

where k_E, k_I, σ_E, and σ_I are constants chosen such that $k_E > k_I$ and $\sigma_I > \sigma_E$; the subscripts E and I stand for excitatory and inhibitory connections. This specification of the w_{ij} produces net mutual inhibition between error network neurons having opposite nominal directions. Together with the cross directional connections of the S network inputs described above, effective subtraction of the RC and S network vectors is achieved.

Finally, the distribution (D) network is composed of 3 sub-networks (D_n), each responsible for movement in a set of directions (D_1: $0, \pi/4$; D_2: $\pi/2, 3\pi/4, 3\pi/2, 7\pi/4$, D_3: $\pi, 5\pi/4$). Only one subnetwork is active during any single movement; this represents a nonlinear effect that is assumed to be physiologically achievable, but is not yet modeled explicitly. The structure of each D_n is similar to that of the KE network. The same method used to assign the RC to KE connection strengths is used to assign those of the KE to D units. The connectivities within the subnetwork are as for the KE network above (equation 4). The output units receive a linear combination of the signals, d_{in}, in the currently active sub-network and channel these to the compensated plant:

$$\dot{\theta}_{s_c} = g_{sn} \sum_i a_i d_{in} \quad (5)$$

$$\dot{\theta}_{e_c} = g_{en} \sum_i b_i d_{in} \quad (6)$$

where the values a_i and b_i are generic for all D_n while the g_{sn} and g_{en} are subnetwork specific scaling factors. These factors were chosen such that the net mapping from KE to output units effectively implement a fixed inverse Jacobian transformation between Cartesian and joint coordinates.

4 Simulation Results and Discussion

Once the values of the synaptic weights had been set, and the values of the g_{sn} and g_{en} had been manually tuned to yield good movement performance, they were fixed for all simulations. No effort was made to rigorously optimize the g_{sn} and g_{en} values. All parameters of the dynamic compensator and plant were held fixed

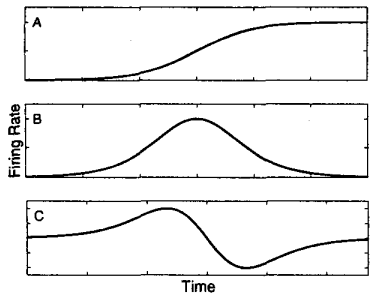

Figure 5: Qualitative appearance of typical sensorimotor cortical neuron firing rate profiles during movement.

as well. The CGRICG-compensator-plant (CGRICG-CP) model was simulated for different movement distances (Figure 6) by changing the amplitude of $X_{h_{ref}}$ and for different tangential hand velocities (Figure 7) by changing its rate of change.

The CGRICG-CP model produces hand trajectories that are qualitatively similar to those observed in human/primate subjects (see [7]). Because of its feedback structure, the simple model is able to achieve fairly straight movements, and therefore effective Cartesian-to-joint coordinate transformation using only relatively coarse tuning at the D network output. Tangential hand velocities in each of the eight movement directions have the characteristic bell-shaped profiles and show that as the movement distance doubles, the peak tangential hand velocity also doubles (Figure 6), as is characteristic of "speed-sensitive" human movements [11] and consistent with the substantial linearity of the system. Another kinematic feature of the CGRICG-CP model is that as in primates/humans, slower hand reaching movements tend to be straighter than fast ones [18](Figure 7). This is expected for an arm controlled by spring-like actuators. However, further simulations (not shown) reveal that dynamics of the CGRICG also contribute to the curvature. This feature in particular awaits experimental validation.

During simulated arm motion, the units of the KE and D networks exhibit activity time courses similar to those of experimentally observed cortical neurons. In particular, both KE and D network neurons' firing rates show bell-shaped and bi-phasic profiles over time (e.g. Figures 5B and C) as has been noted in parietal cortex [5, 13, 14], and in several studies of animal motor cortex [20, 24]. Furthermore, like M1 and other cortical neurons [8], the D network units are seen to be broadly tuned according to hand movement direction. In particular, if each distribution neuron is assigned a "preferred" direction (unit vector) $\hat{\psi}_{d_j}$ based upon the direction of motion for which it fires most strongly[‡], then the population vector of the active subnetwork, $\vec{\nu} = \sum_i d_{in}\hat{\psi}_{d_{in}}$ is found to point roughly in the direction of motion. This is an expected effect resulting from the population vector organization of the RC, S, and KE networks.

The first central feature of the model is that an intended velocity command is proposed to be the principal signal observed at the parietal and motor cortices. This signal is posited to result from approximate differentiation of the intended position command that is achieved by an integrator in negative feedback configuration. To the extent that the cerebellum enables the plant to follow the velocity command, $\dot{\Theta}_c$, Θ_c will be a satisfactory prediction of the true motion Θ. In this case, the integrator functions as a crude (linear) model of the compensated nonlinear plant [17].

The second central feature is that the CGRICG achieves effective inverse kinematic conversion using a distribution network that is only coarsely tuned to direction. Direct inverse kinematic conversion of reference workspace position coordinates to joint coordinates is given by:

$$\theta_{c_e} = \arccos\left(\frac{{r_h}^2 - ({l_s}^2 + {l_e}^2)}{2l_s l_e}\right) \tag{7}$$

$$\theta_{c_s} = \psi_h - \arcsin\left(\frac{l_e}{r}\sqrt{1 - \frac{({r_h}^2 - ({l_s}^2 + {l_e}^2))^2}{4l_s l_e}}\right) \tag{8}$$

(based on Figure 2). This requires quantitatively precise nonlinear processing of both ψ_h and r_h. When the value of these variables is represented by the selection of a unique neuronal unit (or set of units), i.e. a unit coded "map" (e.g [4]), this transformation is easily accomplished to arbitrary precision by nonlinearly weighted connections to a corresponding joint coordinate map at the output. This method is postulated for the forward kinematic transformation N (Figures 3 & 8).

An alternative is to use the differential relationship:

$$\mathrm{d}\Theta_{h_{ref}} = J^{-1}(\Theta)\mathrm{d}X_{h_{ref}} \tag{9}$$

where is the inverse Jacobian which is linear at any given location, Θ. This representation is attractive from the point of view of redundant manipulator control [4] and more generally in terms of its potential use in a feedback loop(Figure 8). Here, A is a scalar and $K(*)$ a nonlinear vector gain used to address inverse kinematic conversion. If $K(*)$ equals $J^{-1}(\Theta)$ then it relates the tracking error, $e = \Delta X_{h_{ref}}$ (approximately $\propto \dot{X}_{h_{ref}}$), to $\Delta\Theta_{h_{ref}}$ (approximately $\propto \dot{\Theta}_{h_{ref}}$). If the

[‡]Because the movement tracking error vector which is registered in the parietal error and motor distribution networks is generally closely aligned with the movement direction, $\hat{\psi} \approx \hat{\xi}$.

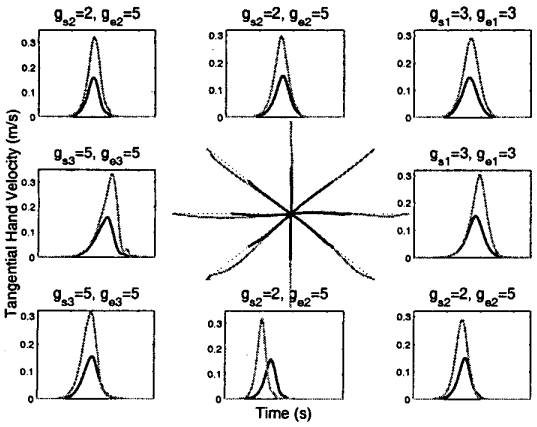

Figure 6: Simulated hand trajectories for movement distances $0.1m$ (black) and $0.2m$ (grey).

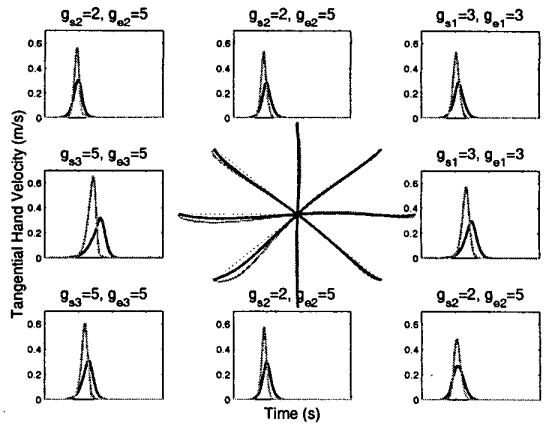

Figure 7: Simulated hand trajectories at two hand speeds for movement distance $0.2m$.

latter signal is then integrated, one obtains a signal $\hat{\Theta}_{h_{ref}}$ which approximates $\Theta_{h_{ref}}$. This approach has been adopted previously in a model of sensorimotor cortical control [23]. It must be noted, however, that this argument is precise only in the limit of high loop gain. For low loop gains, $\hat{\dot{\Theta}}_{h_{ref}}$ and $\hat{\Theta}_{h_{ref}}$ become poor approximations and therefore intended straight movements become somewhat curved.

More specifically, when $A = 1/\Delta t$ and $\Delta t \rightarrow \mathrm{d}\,t$ the argument is exact. Moreover, it holds for arbitrary fixed $K(*)$ so long as $AK(*)$ is stabilizing. Thus, for any given $K(*)$ increasing A yields much straighter movements. This affords a simple mechanism by which usually slightly curved "natural" movements might be straightened at will. Thus, command generator loop gain is possibly another important factor among several that might affect trajectory curvature (see [23]).

Even when A is not large, because the integrator has infinite d-c gain, we always have $\hat{\Theta}_{h_{ref}} \rightarrow \Theta_{h_{ref}}$ as $t \rightarrow \infty$ (again assuming stability). For small A however, $K(*) \approx J^{-1}(\Theta)$ significantly improves the rate of convergence and hence the fidelity of transformation of rapidly changing $X_{h_{ref}}$. Because in a physical system loop gain will be limited by the presence of delays and phase lags, it is likely that the sensorimotor control system would benefit by $K(*)$ at least somewhat near $J^{-1}(\Theta)$. How close is necessary has not yet been determined. However, at least in our studied movements, reasonable control could be achieved by three D_n networks that represented only a very coarse sampling of the inverse Jacobian by gross direction of movement. In particular, the D_n subnetworks do not depend upon limb configuration or hand position as in other proposals [4], while at the same time it has moderate loop gains are unlikely to engender instability for loop delays on the order of milliseconds.

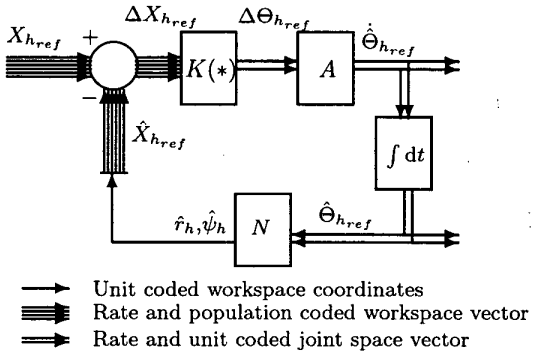

Figure 8: Feedback scheme of the CGRICG.

By directly transforming both vector magnitude and direction the CGRICG potentially yields accurate $\dot{X}_{h_{ref}}$ as well as $X_{h_{ref}}$ which is critical to proper dynamic control. Moreover, by avoiding the use of fine-grained unit-coded maps for vector transformation, the CGRICG requires only 22 gains (g_{sn}, g_{en}, a_i, b_i) to be used for tuning. This directly underlies our ability to tune the network quickly by hand and suggests that an effective and fairly rapid self-tuning algorithm may be achievable. However, this also has not been tested. Finally, as long as the adaptable gains are stabilizing, they may be adjusted freely without compromising the endpoint accuracy. This affords the limb control additional robustness that appears to be physiologically realistic.

5 Conclusions & Future Work

The CGRICG model is preliminary and based on several simplifying assumptions. Still when used to direct a compensated plant, generally plausible trajectories are produced. Furthermore, in the process, the CGRICG module exhibits several of the characteristics of cortical neuron activity such as intensity time course, directional tuning, and population vector coding. We

believe that these results are interesting in light of the CGRICG's simplicity. The model essentially extends related previous models [4, 23] by (1) indicating that effective inverse kinematic transformation can be achieved implicitly using many fewer computational units, (2) directing attention to dynamic considerations involved in this method of coordinate conversion and their potential impact on path deviations. However, simulations included only relatively short movements, neglected signal transmission delays, and involved no actuator redundancy or external loads. The paths have not been compared systematically with experimentally recorded human hand paths. Certain proposed neuronal population behaviors have not been established and the CGRICG is not yet self-tuning. Therefore, considerable further analysis and experimental validation will be needed to understand motor cortical operation.[§]

Appendix

Effective net angular stiffness R (N-m/rad) and angular viscosity D (N-m-sec/rad) of the limb including effects of dynamic compensation provided by the cerebellum. Values are consistent with physiological measurements [10].

$$R = \begin{bmatrix} 25 & 2 \\ 2 & 10 \end{bmatrix} \quad D = \begin{bmatrix} 5 & 1 \\ 1 & 2 \end{bmatrix}$$

Limb lengths were taken to be $l_s = l_e = 0.3$m. Limb masses were taken to be $m_s = m_e = 0.65$Kg.

References

[1] G. I. Allen and N. Tsukahara. Cerebrocerebellar communication systems. *Physiological Review*, 54:957–1006, 1974.

[2] E. Bizzi, N. Hogan, F. A. Mussa-Ivaldi, and G. S. Does the nervous system use equilibrium-point control to guide single and multiple joint movements? In P. Cordo and S. R. Harnad, editors, *Movement Control*, pages 1–11. Cambridge University Press, Cambridge, England, 1994.

[3] V. Brooks. *The Neural Basis of Motor Control.* Oxford University Press, Oxford, 1986.

[4] D. Bullock, S. Grossberg, and F. H. Guenther. A self-organizing neural model of motor equivalent reaching and tool use by a multijoint arm. *Journal of Cognitive Neuroscience*, 5(4):408–435, 1993.

[5] P. Burbaud, C. Doegle, C. Gross, and B. Bioulac. A quantitative study of neuronal discharge in areas 5, 2, and 4 of the monkey during fast arm movements. *Journal of Neurophysiology*, 66(2):429–443, Aug. 1991.

[6] A. G. Feldman and M. F. Levin. The origin and use of positional frames of reference in motor contro. *Behavioral and Brain Sciences*, 19:723–806, 1995.

[7] T. Flash. The control of hand equilibrium trajectories in multi-joint arm movements. *Biological Cybernetics*, 57:257–274, 1987.

[8] A. P. Georgopoulos, R. E. Kettner, and A. B. Schwartz. Primate motor cortex and free arm movements to visual targets in three-dimensional space II. coding of the directions of movements by a neuronal population. *Journal of Neuroscience*, 8:2928–2937, 1988.

[9] A. P. Georgopoulos, M. Taira, and A. V. Lukashin. Cognitive neurophysiology of the motor cortex. *Science*, 260:47–52, 1993.

[§]We would like to thank Jean-Jacques E. Slotine for underscoring the potential utility of velocity-based coordinate transformation.

[10] H. Gomi and M. Kawato. Equilibrium-point control hypothesis examined by measured arm stiffness during multi-joint movement. *Science*, 272:117–120, 1996.

[11] G. L. Gottlieb, D. M. Corcos, and G. C. Agarwal. Organizing principles for single-joint movements. II. speed-sensitive strategy. *Journal of Neurophysiology*, 62:358–368, 1989.

[12] J. Houk, J. Keifer, and A. Barto. Distributed motor commands in the limb premotor network. *Trends in Neuroscience*, 16:27–33, 1993.

[13] J. F. Kalaska, R. Caminiti, and A. P. Georgopoulos. Cortical mechanisms related to the direction of two-dimensional arm movements: Relations in parietal area 5 and comparison with motor cortex. *Experimental Brain Research*, 51:247–260, 1983.

[14] J. F. Kalaska, D. A. D. Cohen, M. Prud'homme, and M. L. Hyde. Parietal area 5 neuronal activity encodes movement kinematics, not movement dynamics. *Experimental Brain Research*, 80:351–364, 1990.

[15] M. Katayama and M. Kawato. Virtual trajectory and stiffness ellipse during multijoint arm movement predicted by neural inverse models. *Biological Cybernetics*, 69:353–362, 1993.

[16] F. Lacquaniti, E. Guigon, L. Bianchi, S. Ferraina, and R. Caminiti. Representing spatial information for limb movement: Role of area 5 in the monkey. *Cerebral Cortex*, 5:391–409, 1995.

[17] S. G. Massaquoi. *Modelling the function of the cerebellum in scheduled linear servo control of simple horizontal planar arm movements.* PhD dissertation, Massachusetts Institute of Technology, Laboratory of Information and Decision Systems, June-Aug. 1999.

[18] S. G. Massaquoi and M. Hallett. Kinematics of initiating a two-joint arm movement in patients with cerebellar ataxia. *Canadian Journal of Neurological Science*, 23:3–14, 1996.

[19] S. G. Massaquoi and J.-J. E. Slotine. The intermediate cerebellum may function as a wave-variable processor. *Neuroscience Letters*, 215:60–64, 1996.

[20] E. M. Maynard, N. G. Hatsopoulos, C. L. Ojakangas, B. D. Acuna, J. N. Sanes, N. R. A., and J. P. Donoghue. Neuronal interactions improve cortical population coding of movement direction. *Journal of Neuroscience*, 19(18):8083–8093, 1999.

[21] J. McIntyre and E. Bizzi. Servo hypotheses for the biological control of movement. *Journal of Motor Behavior*, 25(3):193–202, 1993.

[22] R. C. Miall, D. J. Weir, D. M. Wolpert, and J. F. Stein. Is the cerebellum a smith predictor? *Journal of Motor Behavior*, 25(3):203–216, 1993.

[23] D. Micci-Barreca and F. H. Guenther. A modeling study of potential sources of curvature in human reaching movements. *Journal of Motor Behavior*, 33(4):387–400, 2001.

[24] D. W. Moran and A. B. Schwartz. Motor cortical representation of speed and direction during reaching. *Journal of Neurophysiology*, 82:2676–2692, 1999.

[25] N. Schweighofer, M. Arbib, and M. Kawato. Role of the cerebellum in reaching movements in humans. I. distributed inverse dynamics control. *European Journal of Neuroscience*, 10:86–94, 1998.